ARKIV FÖR FYSIK Band 18 nr 38

Communicated 1 June 1960 by E. Hulthén

Rotational analysis of the absorption spectrum of carbon monosulphide

By R. F. Barrow,[1] R. N. Dixon,[2] A. Lagerqvist[3] and C. V. Wright[1]

With 10 figures in the text

ABSTRACT

A study has been made of the rotational structure in the ultra-violet absorption spectrum of carbon monosulphide, produced by flash photolysis of carbon disulphide. The bands observed consist of the 0–0, 1–0 and 2–0 bands of the $A\,^1\Pi$–$X\,^1\Sigma^+$ system, three bands of a new system, $a^*\,(\Pi)$–$X\,^1\Sigma^+$, and also bands of two forbidden systems, $a'\,^3\Sigma^+$, $e\,^3\Sigma^-$–$X\,^1\Sigma^+$. The presence of these excited states had earlier been inferred from the analysis of perturbations in the $A\,^1\Pi$–$X\,^1\Sigma^+$ system as observed in emission: however the direct observation of lines arising from the forbidden transitions in absorption provides a unique opportunity of testing the theory of the mutual interaction of molecular states. The $a'\,^3\Sigma^+$, $A\,^1\Pi$ perturbation shows detailed agreement with theoretical predictions: some unsolved problems in the $e\,^3\Sigma^-$, $A\,^1\Pi$ interaction remain.

Introduction

A detailed rotational analysis of the emission spectrum of the CS molecule [4] showed that the main feature in the spectrum in the spectral region photographable in air is an ultra-violet system, $A\,^1\Pi$–$X\,^1\Sigma^+$. As had been recognized in earlier analysis, the upper state is subject to extensive perturbations, whose structure reveals the presence of several nearby states, in particular, two triplet states $a'\,^3\Sigma^+$ and $e^3\Sigma^-$.

The significance of this spectrum is twofold: on the one hand, it is important to trace the similarities and differences between the excited states of similar molecules, and in this instance it is desirable to find out whether the presence of the $3d$ electron shell in sulphur leads to observable differences between the excited states of CO and CS. On the other hand, the perturbations in the CS spectrum are so strong and so numerous that their study is itself of interest.

For these reasons we have now extended this work to an examination of the spectrum of CS as observed in absorption. The main advantage of absorption over emission work is that whereas the emission spectrum is complicated by the development of large numbers of bands so that sequences overlap, the strong absorption bands arise only from $v''=0$. The absorption spectrum is thus a drastic simplification of the emission spectrum.

In it are observed directly lines not only of the well-known transition $A\,^1\Pi$–$X\,^1\Sigma^+$, but also of transitions $a^*(\Pi)$–$X\,^1\Sigma^+$, $a'\,^3\Sigma^+$–$X\,^1\Sigma^+$ and $e\,^3\Sigma^-$–$X\,^1\Sigma^+$, whose upper states had earlier been recognized only through their effects on the levels in $A\,^1\Pi$. This observation of the levels of pairs of interacting states provides a unique opportunity for testing perturbation theory. The determination of the properties of the spectroscopic states themselves strengthens the analogies between the spectra of CS and of CO, SiO and SiS.

---

[1] Physical Chemistry Laboratory, Oxford University.

[2] Division of Pure Physics, National Research Council, Ottawa, Canada.

[3] Institute of Physics, University of Stockholm.

Experimental

Carbon disulphide at a pressure of 10 cm Hg was photolyzed by the flash from four lamps through each of which the charge from a 33 μF condenser at 7 kV was passed simultaneously. S_2 bands appeared immediately after photolysis, and exposures were therefore delayed by at least 15 seconds. Two traversals of the absorption tube were used, making the effective path length 1.2 m. Exposure times of between 30 seconds and 1 minute from a xenon high-pressure lamp sufficed for photographs in a fourth order of a 6.5 m grating spectrograph on Kodak 103a O plates, using a fore prism to separate the orders. The effective resolving power on the plates was about 165 000.

The plates were taken by R.N.D. in the spectroscopic laboratories of the Division of Pure Physics, National Resarch Council, Ottawa, and were measured and analyzed independently in Stockholm and Oxford.

Analysis

The strong bands of the ultra-violet absorption spectrum of CS lie in the region 2490 to 2600 Å. In these experiments the effective temperature of the absorbing gas was comparatively low, so that all the bands observed arise from $v''=0$: the general appearance of the absorption spectrum is thus quite different from that of the emission spectrum. A summary of the transitions is given in Fig. 1. Several of the bands are of unusual structure, and in many regions extensive perturbations are evident. The analyses are given in Tables 2 to 6, in the form of term values, referred to $v''=0$, $J''=0$, in $X\,^1\Sigma^+$, using rotational terms (Table 1) calculated with $B_0''=0.817083$ cm^{-1} (ref. [5]), and $D_0''=1.336\times10^{-6}$, derived from Kratzer's expression. The designations of the branches given throughout the tables are those appropriate for the lowest values of J. Before proceeding to a discussion of the band structure, it will be helpful to give a brief summary of the relevant theory of the interactions between electronic states.

An interaction between two states is illustrated in Fig. 2, where the total energy is given as a function of $J(J+1)$. Observed rotational lines arise from the perturbed terms (drawn with thick lines). The values of B vary with J, and differ from those of the unperturbed levels. Observed values of ν_0 also differ from the hypothetical, unperturbed values (by an amount ε). We will use T_i, ν_0, B ... to describe observed levels and T_i^*, ν_0^*, B^* ... to describe hypothetical, unperturbed values.

For various reasons it is desirable to determine the hypothetical, unperturbed values B^* and ν_0^*. We consider here only the case in which two electronic states interact: this will generally be an adequate approximation, although some instances arise where more than two states lie close together. Furthermore, we are mainly concerned here with terms for which $J\lesssim 30$, and we therefore neglect the small corrections for centrifugal stretching.

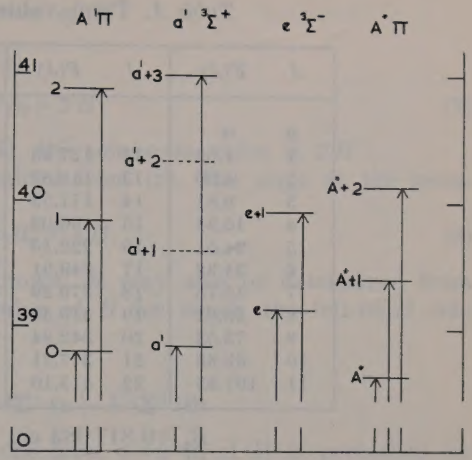

Fig. 1. Transitions observed in the absorption spectrum of CS. In this figure, A^* should be replaced by a^*.

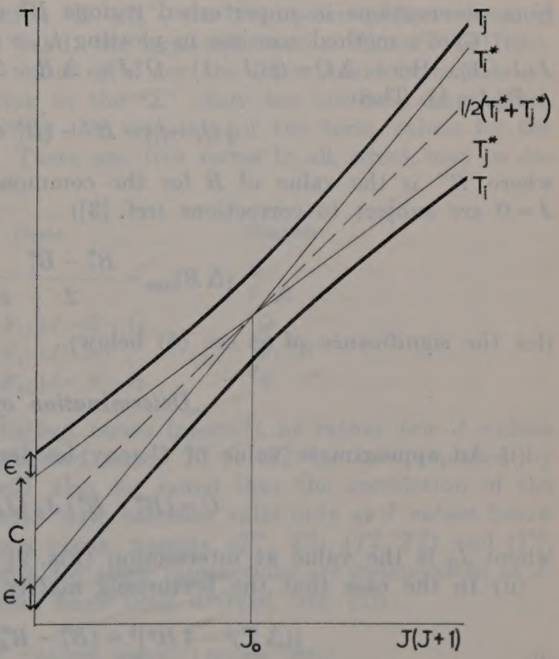

Fig. 2. An interaction between two singlet states. The total energy is given as a function of $J(J+1)$.

Determination of B

(i) The mean value, $\frac{1}{2}\{T_i(J) + T_j(J)\}$, is equal to

$$(T_i + T_j)/2 = \nu^*_{0,i} + C/2 + (B^*_i + B^*_j)\,J\,(J+1)/2 \ldots \tag{1}$$

Table 1. Term values for $v''=0$, $X\,{}^1\Sigma^+$.

J	$F(J)$	J	$F(J)$	J	$F(J)$	J	$F(J)$
0	0						
1	1.63	12	127.43	23	450.62	34	970.44
2	4.90	13	148.67	24	489.77	35	1027.40
3	9.81	14	171.53	25	530.54	36	1085.98
4	16.34	15	196.02	26	572.94	37	1146.18
5	24.51	16	222.15	27	616.95	38	1207.98
6	34.32	17	249.91	28	662.59	39	1271.40
7	45.75	18	279.29	29	709.85	40	1336.42
8	58.82	19	310.30	30	758.73	41	1403.06
9	73.53	20	342.94	31	809.23	42	1471.30
10	89.86	21	377.21	32	861.35	43	1541.14
11	107.83	22	413.10	33	915.09	44	1612.59

$B_0 = 0.817\,083\ \mathrm{cm}^{-1}$; $D = 1.336\times10^{-6}$

Thus the slope of the dashed line in Fig. 2 is $(B_i^* + B_j^*)/2$. If B_i^* or B_j^* is known from observations in unperturbed regions B_j^* or B_i^*, can be determined.

(ii) Gerö's method consists in plotting $f_{i,j} \equiv \Delta Q/2J$ or $(\Delta R + \Delta P)/4J$ against $J(J+1)$. Here $\Delta Q = Q(J-1) - Q(J)$, $\Delta R + \Delta P = R(J-2) - R(J-1) + P(J) - P(J+1)$. Then

$$\tfrac{1}{2}(f_i + f_j) = B'' - (B_i^* + B_j^*)/2, \tag{2}$$

where B'' is the value of B for the common lower state. Values of B_i, B_j at $J=0$ are subject to corrections (ref. [3])

$$(\Delta B)_{\mathrm{corr}} = \frac{B_i^* - B_j^*}{2} \cdot \frac{\varepsilon}{\varepsilon + C/2} \tag{3}$$

(for the significance of ε, see (6) below).

Determination of C

(i) An approximate value of C may be derived from

$$C = (B_i^* - B_j^*)\, J_0\,(J_0 + 1), \tag{4}$$

where J_0 is the value at intersection (Fig. 2).

(ii) In the case that the perturbing matrix element H is known (see below),

$$[(\Delta T)^2 - 4H^2]^{\frac{1}{2}} = (B_i^* - B_j^*)\, J(J+1) + C \tag{5}$$

C is obtained as the intercept at $J=0$ on plotting the left-hand side of (5) against $J(J+1)$.

(iii) The correction term ε (see Fig. 2) is given by

$$\varepsilon = \frac{C}{2}\left[(1 + 4H^2/C^2)^{\frac{1}{2}} - 1\right] \tag{6}$$

Determination of H

(i) At the intersection point J_0 (Fig. 1),

$$(T_i)_0 - (T_j)_0 = 2H \tag{7}$$

In a plot of $\Delta T_{i,j}$ against J or $J(J+1)$, the minimum value is $2H$.

(ii) A rough value of H may be obtained from (2). The slope at the intersection point is [3]

$$|\eta| = (B_1^* - B_2^*)^2/4H. \tag{8}$$

(iii) If a range of values of ΔT is known, H may also be determined from (5), by finding, by trialanderror, that value of H for which the left-hand side of (5) is linear in $J(J+1)$.

Bands $A\,{}^1\Pi(0)$, $a'\,{}^3\Sigma^+(a')$–$X\,{}^1\Sigma^+(0)$

In our earlier work, we found that the level $v=0$ in $A\,{}^1\Pi$ is perturbed by a ${}^3\Sigma^+$ state. However, whereas in the emission spectrum, overlapping by lines of other bands of the A–X system makes it impossible to pick out the branches arising from the forbidden transition ${}^3\Sigma^+$–${}^1\Sigma^+$, the absorption plates reveal, in addition to the $A\,{}^1\Pi(0)$–$X\,{}^1\Sigma^+(0)$ band, the expected band $a'\,{}^3\Sigma^+(a')$–$X\,{}^1\Sigma^+(0)$, with considerable intensity. The value of v' for the latter band is written a', since the true vibrational numbering in the ${}^3\Sigma^+$ state has not been determined.

In Fig. 3 is illustrated qualitatively the variation of the term values for the ${}^1\Pi$ and ${}^3\Sigma^+$ states with $J(J+1)$. There are five terms in all, which may be designated for convenience as follows:

Term	State	Branch
T_1	${}^1\Pi$	Q
T_2	${}^1\Pi$	P, R
T_3	${}^3\Sigma^+, F_1$: $(J=N+1)$	${}^PQ$
T_4	${}^3\Sigma^+, F_2$: $(J=N)$	${}^PP$, ${}^RR$
T_5	${}^3\Sigma^+, F_3$: $(J=N-1)$	${}^RQ$

In the present case, the unperturbed terms intersect at rather low J values (about 15, 17 and 21): the unperturbed terms $T_1^* \ldots T_5^*$ are now replaced by perturbed terms $T_1 \ldots T_5$. (It will also be noted that the correlation of the terms with the branches given above now becomes valid only at J values below the perturbation.) Three interactions occur, namely (T_1^*, T_3^*), (T_2^*, T_4^*) and (T_1^*, T_5^*). The perturbing matrix elements for these interactions are independent of J: the following relations between them have been derived (ref. [2]):

$$|H(T_1^*, T_3^*)| = \frac{1}{\sqrt{2}}|H(T_2^*, T_4^*)| = |H(T_1^*, T_5^*)| \tag{9}$$

At the intersection points (see Fig. 3), we have

$$|T_1 - T_3| = 2|H(T_1^*, T_3^*)|, \tag{10a}$$

$$|T_2 - T_4| = 2|H(T_2^*, T_4^*)|, \tag{10b}$$

$$|T_1 - T_5| = 2|H(T_1^*, T_5^*)|. \tag{10c}$$

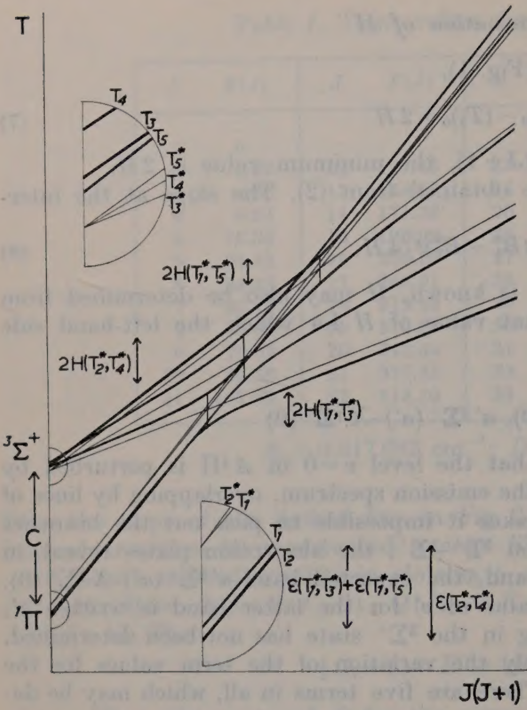

Fig. 3. Interaction of the levels of a $^3\Sigma$ state with those of a $^1\Pi$ state.

Whereas (10 b) is always valid, provided that the effects of other perturbing states are negligible, (10 a) and (10 c) are valid only when the perturbations (T_1^*, T_3^*) and (T_1^*, T_5^*) do not interact with each other, i.e. when H is small.

As can be seen from Fig. 4 and Table 2, all seven branches have been found, not only at low and high J values, where the effects of the perturbations are rather small, but also throughout the whole of the perturbed regions. The perturbations are illustrated in Fig. 5, where the term values are plotted against $J(J+1)$. Fig. 6 shows the central perturbation on a larger scale, obtained by subtracting $\frac{1}{2}[B^*(3\Sigma) + B^*(^1\Pi)]J(J+1)$ from T_2 and T_4.

Determinations of constants for $a'\,^3\Sigma^+$, $v = a'$

On account of the perturbations, the course of the F_1 and F_3 levels in the $^3\Sigma^+$ state is not simple, and we use therefore only the F_2 levels to determine the constants of this state.

(i) $B(^3\Sigma^+, v = a')$. From (1), with $B^*(^1\Pi, v = 0) = 0.7767$ cm^{-1} (ref. [4]), $B^*(^3\Sigma^+) = 0.5833$ cm^{-1}.

The relation (2) is illustrated in Fig. 7: from it is obtained $B^*(^3\Sigma^+) = 0.5839$ cm^{-1}. The mean value is $B^*(^3\Sigma^+) = 0.5836$ cm^{-1}

(ii) $H(^3\Sigma^+, {}^1\Pi)$. The differences $\Delta T_{3.1}$, $\Delta T_{4.2}$ and $\Delta T_{5.1}$ are illustrated in Fig. 8. Using (5) and (7), we obtain $2|H(T_2^*, T_4^*)| = 11.0$ cm^{-1} and $\frac{1}{2}\{2|H(T_1^*, T_3^*)| + 2|H(T_1^*, T_5^*)|\} = 7.8$ cm^{-1}. The ratio $11.0/7.8 = 1.41$ is in excellent agreement with the theoretically predicted value (9) of $\sqrt{2}$.

Table 2. Term values for $A\,{}^1\Pi$, $(v=0)$ and $a'\,{}^3\Sigma^+$, $(v=a')$ referred to $J=0$, $v=0$ in $X\,{}^1\Sigma^+$.

	$A\,{}^1\Pi$			$a'\,{}^3\Sigma^+$		$A\,{}^1\Pi$	$a'\,{}^3\Sigma^+$	
		F_{RP}		F_2		F_Q	F_3	F_1
J	Branch	R	P	^RR	^PP	Q	^RQ	^PQ
0		—	—					
1		38 798.72	98.67*	38 853.57				
2		801.65*	01.74*	55.92*		38 801.74		
3		06.35	06.39	59.40*	59.46	06.37		
4		12.55	12.58*	64.10*	64.13	12.58		
5		20.30	20.26	69.91	70.00	20.24*		
6		29.48	29.52	77.08	77.02	29.53	38 886.43	38 870.89
7		40.32	40.30	85.32	85.26	40.25	95.75	78.13
8		52.60	52.64	94.72	94.75	52.59*	906.34	86.34
9		66.44	66.50	905.38	05.37	66.44	18.07	95.82
10		81.84	81.86	17.19	17.13*	81.79*	31.05	906.27*
11		98.73	98.81	30.20	30.17	98.60*	45.14	18.32
12		917.13*	17.22	44.40	44.40*	916.85	60.48	31.41
13		37.15*	37.05	59.81*	59.64	36.19	76.77	46.65*
14		58.39*	58.34*	76.77*	76.72	55.91	94.67	63.84
15		80.83*	80.82	95.05	95.08	74.78	39 013.46	84.80
16		39 003.96	04.02*	39 015.40	15.43	93.24*	33.34*	39 008.64*
17		27.12*	27.09	38.57*	38.62	39 012.23*	54.92	34.25
18		49.93*	49.84	64.80	64.76*	32.23	77.27*	61.93
19		73.06*	72.94*	93.43	93.42	53.48	101.12	90.66*
20		96.79*	96.75	123.99	23.96	75.84	27.56	119.90
21		121.36	21.58	56.25	56.28	98.67	57.60	48.33*
22		47.61*	47.48	90.18	90.19*	122.89	90.81	76.05
23		74.38	74.54	225.66	25.74		226.07	204.73*
24		202.67		62.81	62.84		63.03	33.99
25				301.47	01.50		301.66	64.58
26				41.70*	41.74		41.86	
27				83.51	83.53		83.60	
28				426.67	26.86		426.91	
29				71.79	71.78		71.88	
30				518.12	18.11		518.06*	
31				66.35	66.14		66.19	
32					615.67		615.81*	
33					66.69		66.69	
34					719.22		719.23	
35					73.23		73.29	
36					828.77		828.88	
37					85.85		85.72*	
38					944.31		44.52	
39					40 004.20		40 004.57	
40					65.35		66.25	
41					127.81		128.90	
42					90.06		93.23*	
43							258.63	
44							324.75	

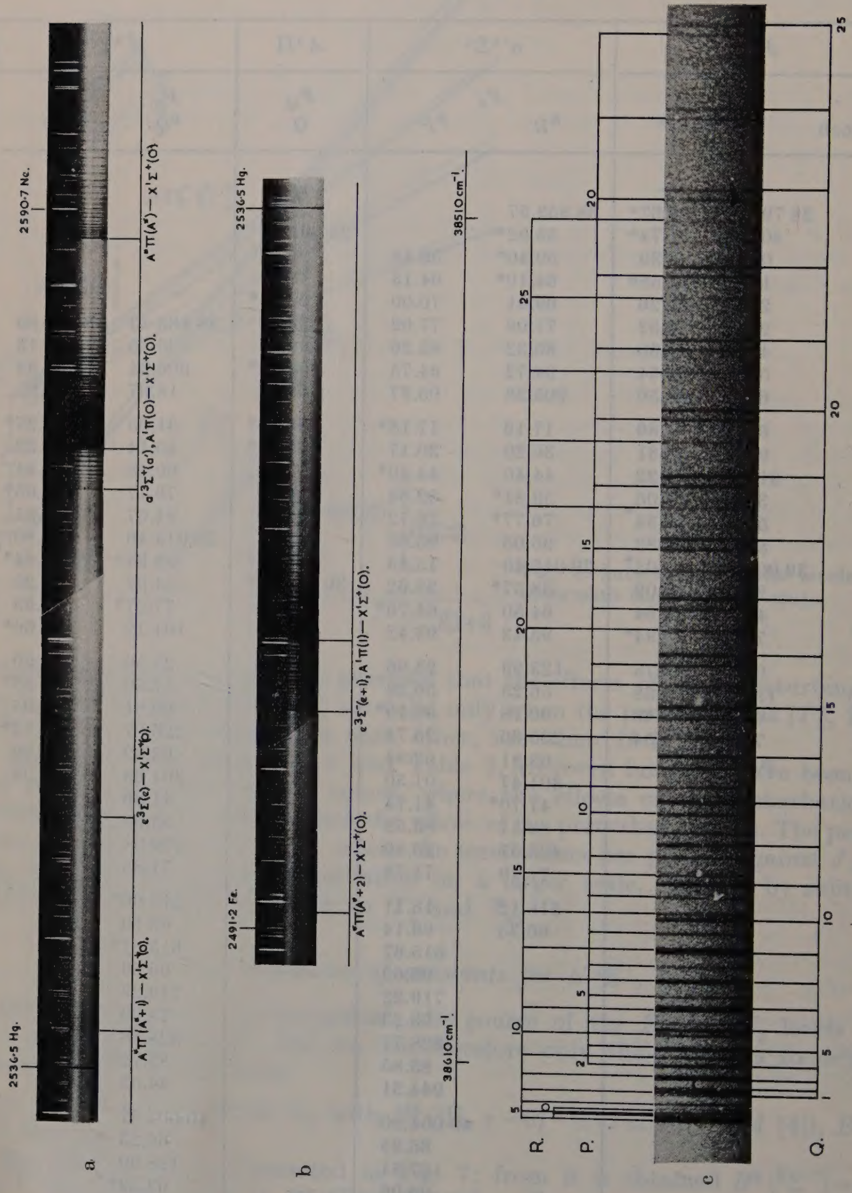

Fig. 4. The absorption spectrum of CS. (*a*) and (*b*). A general survey of the spectrum observed. (*c*) The $a^*\,\Pi(a^*)-X\,{}^1\Sigma^+(0)$ band. In (*a*) and (*b*), A^* should be replaced by a^*.

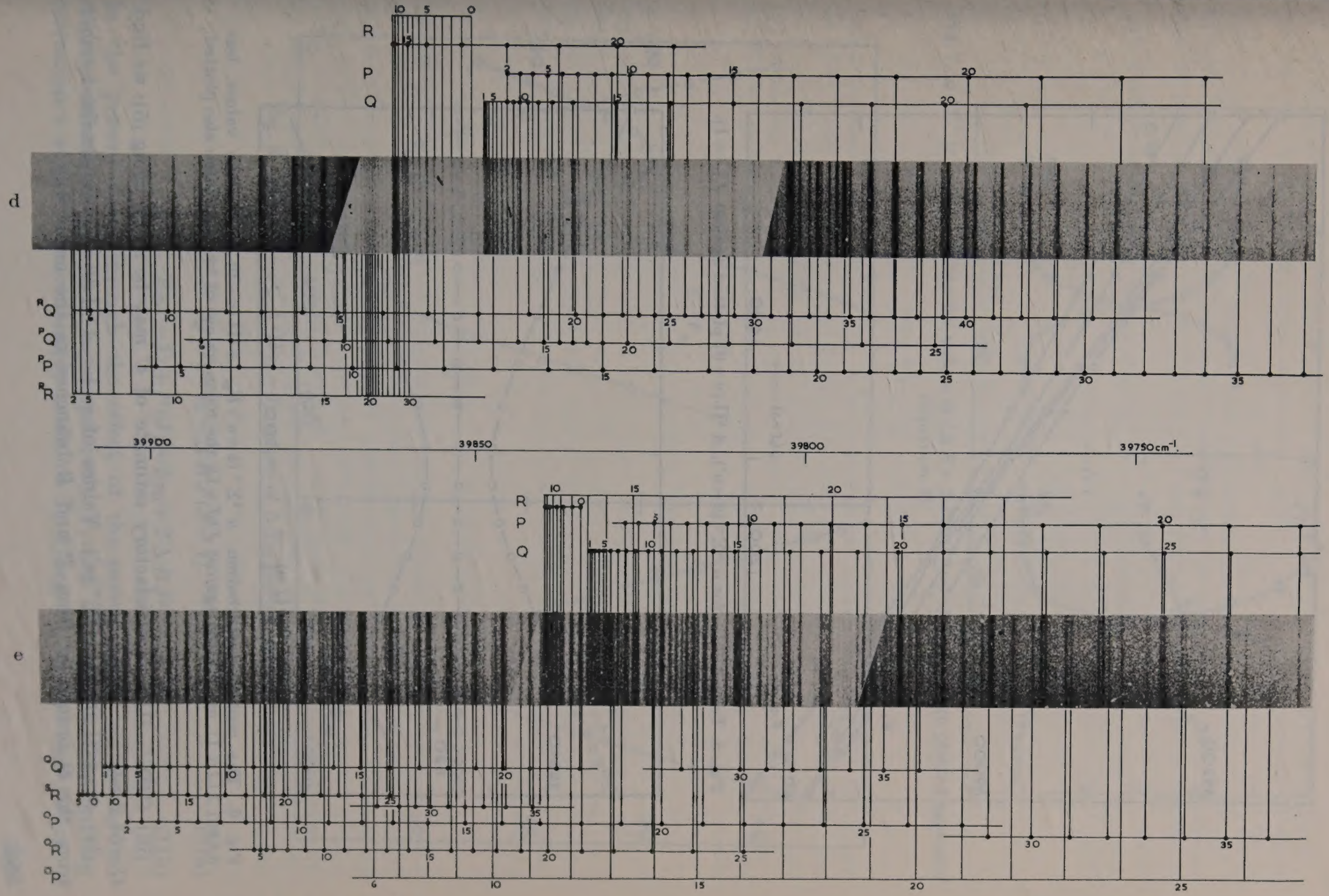

Fig. 4. (*d*) The $a'\,^3\Sigma^+(a')$, $A\,^1\Pi(0)$–$X\,^1\Sigma^+(0)$ bands. (*e*) The $e\,^3\Sigma^-$ $(e+1)$, $A\,^1\Pi(1)$–$X\,^1\Sigma^+(0)$ bands.

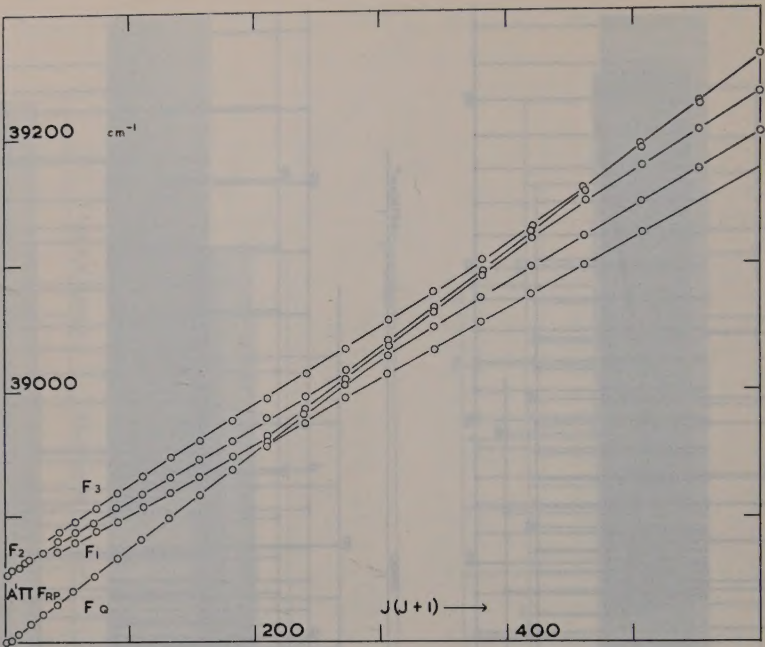

Fig. 5. Term values for $a'\,{}^3\Sigma^+$ ($v = a'$), $A\,{}^1\Pi$ ($v = 0$) plotted against $J\,(J+1)$.

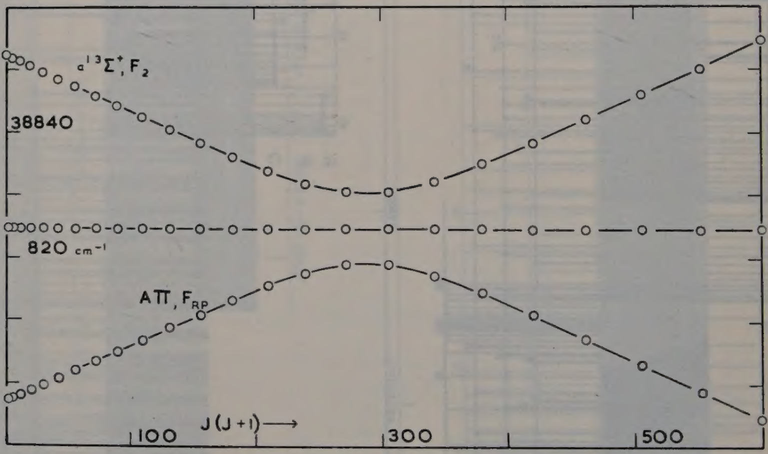

Fig. 6. The central perturbation, $a'\,{}^3\Sigma^+\,(v = a')\,F_2$, $A\,{}^1\Pi\,(v = 0)\,F_{RP}$. Term values, less 0.6801 $J\,(J+1)$, are plotted against $J\,(J+1)$; the mean values of two terms are also plotted.

(iii) $C\,({}^3\Sigma^+, {}^1\Pi)$. A satisfactory estimate of C may be made using (5): we find $C = 54.2$ cm^{-1}.

(iv) ν_0, $A\,{}^1\Pi\,(0)$; ν_0, $a'\,{}^3\Sigma^+\,(a')$. Values of ν_0 for $A\,{}^1\Pi\,(0)$ may be obtained either from the Q branch or from P and R branches in the usual way:

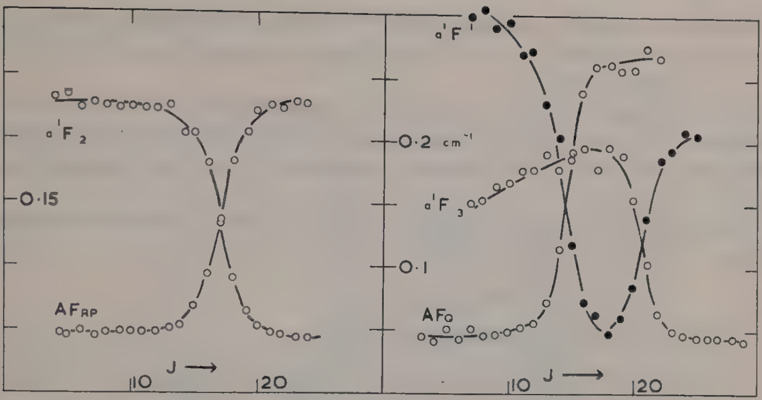

Fig. 7. $a'\,^3\Sigma^+$ $(v=a')$, $A\,^1\Pi$ $(v=0)$: values of $(\Delta R+\Delta P/4J$ and of $\Delta Q/2J$ are plotted against J (equation 2).

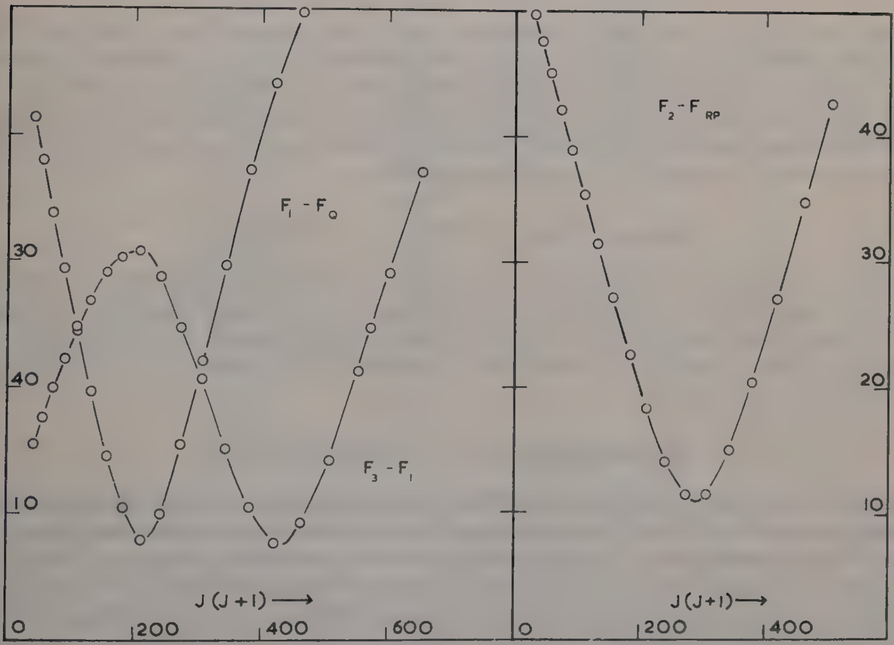

Fig. 8. $a'\,^3\Sigma^+$ $(v=a')$, $A\,^1\Pi$ $(v=0)$: values of ΔT_{ij} plotted against $J\,(J+1)$.

$$Q\,(J)=\nu_0+\Delta\,B\,J\,(J+1) \tag{11a}$$

$$R\,(J-1)+P\,(J)=2\,\nu_0+2\,\Delta\,B\,J^2 \tag{11b}$$

In the present case, through the effect of the perturbations, we obtain two slightly different estimates of ν_0, respectively T_1 and T_2 at $J=0$. The limiting correction ε at $J=0$ is most simply made for T_2. Using (6), we find $\varepsilon=0.55$ cm^{-1}.

From (11b) we derive $\nu_0 = 38\,797.0_5$ cm^{-1}: the corrected value is then $\nu_0^*(A\,{}^1\Pi) = 38\,797.0_5 + 0.55 = 38\,797.6$ cm^{-1}. The corrected value for $a'\,{}^3\Sigma^+(a')$ is simply $38\,797.6 + C = 38\,851.8$ cm^{-1}.

(v) $B_0\,(A\,{}^1\Pi)$. From (11b) we obtain $\Delta B = 0.0420$ cm^{-1}, or $B = 0.7751$ cm^{-1}. The correction term (3) amounts to $+0.0018$ cm^{-1}, so that $B^*\,(\Pi) = 0.7769$ cm^{-1}, in good agreement with the value 0.7767 cm^{-1} in ref. [4] from unperturbed lines at high values of J.

An estimate of the spin-splitting in $a'\,{}^3\Sigma^+\,(a')$ can be obtained as follows. The term values T_1^*, T_3^*, T_5^* are given by:

$$T_1^* = \nu_0^* + B_\Pi^* J\,(J+1)$$
$$T_3^* = \nu_0^* + C + B_\Sigma^* J(J-1) - 2\lambda + \gamma J$$
$$T_5^* = \nu_0^* + C + B_\Sigma^*\,(J+1)\,(J+2) - 2\lambda - \gamma\,(J+1).$$

Provided that the effects of other perturbations can be neglected,

$$T_1 + T_3 + T_5 = T_1^* + T_3^* + T_5^*.$$

Values of $(4\lambda + \gamma)$ may then be obtained from the sum of the observed terms and the values of ν_0^*, C, B_Π^* and B_Σ^*. We obtain $(4\lambda + \gamma) = -3.6$ cm^{-1}, close to the value, -4.52 cm^{-1}, for $(4\lambda + 2\gamma)$ found for the state $a'\,{}^3\Sigma^+$ in CO [1].

It must be stressed that in the determination of the constants above, no regard has been paid to the effects of other perturbing states. However, as will be shown below, the state a^* also interacts with A.

Bands $A\,{}^1\Pi\,(2)$, $a'\,{}^3\Sigma^+\,(a'+3)$–$X\,{}^1\Sigma^+\,(0)$

The 2–0 band of A–X appears, but with rather low intensity in the absorption spectrum. At higher frequency lie some very weak lines which appear to belong to the band $a'\,{}^3\Sigma^+\,(a'+3)$–$X\,{}^1\Sigma^+\,(0)$. The analysis of the $A\,{}^1\Pi\,(2)$–${}^1\Sigma^+\,(0)$ band is given in Table 3. Interactions between $A\,{}^1\Pi\,(2)$ and $a'\,{}^3\Sigma^+\,(a'+3)$ occur at $J \sim 21$, 23 and 27.

Determination of ν_0^*, $A\,{}^1\Pi\,(2)$–$X\,{}^1\Sigma^+\,(0)$

From (11b), $\nu_0 = 40\,881.5_0$ cm^{-1}. This value must be corrected for the rather strong interaction with a'. The application of (6) requires a knowledge of both C and H: estimates of these quantities can be obtained as follows. From the present work and from [4], $B_{a'+3}^*\,({}^3\Sigma^+) \sim 0.559$, $B^*(2) = 0.7617$ cm^{-1}. The culmination of the perturbation in R and P branches is at $J \sim 22.5$. Thus $C \sim 106$ cm^{-1}. From (8), $2H \sim 36$ cm^{-1}. Thus $\varepsilon \sim 0.8$ cm^{-1}, and $\nu_0^* = 40\,881.5_0 + 3 = 40\,884 \cdot 5$ cm^{-1}, and $\nu_0^*(a'+3) \sim 40\,988$ cm^{-1}.

Bands $A\,{}^1\Pi\,(1)$, $e\,{}^3\Sigma^-\,(e+1)$–$X\,{}^1\Sigma^+\,(0)$

The level $v' = 1$ in $A\,{}^1\Pi$ is very strongly perturbed at low J values by a ${}^3\Sigma^-$ state. To conform with the designation of the states of CO, this state is called $e\,{}^3\Sigma^-$, and, since the correct numbering is unknown, we write $v = e + 1$. (The band e–0 is observed at longer wavelengths: see below.) It was not possible to carry out the analysis of $A\,{}^1\Pi\,(1)$ at low values of J from the emission plates, and no

Table 3. Term values for $A\,^1\Pi$, $(v=2)$ referred to $J=0$, $v=0$ in $X\,^1\Sigma^-$.

J	F_Q	F_{RP}	
Branch	Q	R	P
1	40 883.11	83.00	
2	86.06	86.02	
3	90.62	90.66	
4	96.65	96.52	96.78*
5	904.29	04.21	04.24
6	13.38	13.37	13.42
7	23.98	24.01	24.09
8	36.16	36.18*	36.29
9	49.83	49.86	49.87
10	64.96	64.92	65.01
11	81.62	81.66*	81.65
12	99.79*	99.86*	99.84
13	41 019.44	19.46*	19.51
14	40.50	40.70*	40.67
15	63.07	63.33*	63.27
16	86.98	87.41*	87.30
17	112.11	12.58*	12.58
18	38.34	39.25	39.33
19	65.20	67.16*	66.94
20	92.13	95.74	95.84
21	241.03	24.75	24.87
22	71.26*	53.93	53.85
23	304.01		
24			
25	97.59		
26	431.10		
27	67.36		
28	506.76		
29	49.35		
30	94.63		
31	641.13		
32	89.54		

lines arising from $^3\Sigma^-$ were assigned. A complete analysis of the two bands has now been carried out from the absorption plates (see Fig. 4). The term values are given in Table 4, and are plotted against $J\,(J+1)$ in Fig 9. The three interactions $^1\Pi$, $^3\Sigma^-$ occur at about $J=14$, 17 and 21.

On account of the $\pm$ symmetry in $^3\Sigma^-$, the biggest perturbation in $^1\Pi$ appears in the Q-branch. Fig. 3, which illustrates a $^1\Pi$, $^3\Sigma^+$ interaction, gives also the structure of a $^1\Pi$, $^3\Sigma^-$ taking due account of the change in $\pm$ symmetry. Again there are five terms in all, designated for convenience, as follows:

Term	State	Branch
T_1	$^1\Pi$	P, R
T_2	$^1\Pi$	Q
T_3	$^3\Sigma^-$, $F_1\,(J=N+1)$	^OP, ^QR
T_4	$^3\Sigma^-$, $F_2\,(J=N)$	^QQ
T_5	$^3\Sigma^-$, $F_3\,(J=N-1)$	^QP, ^SR

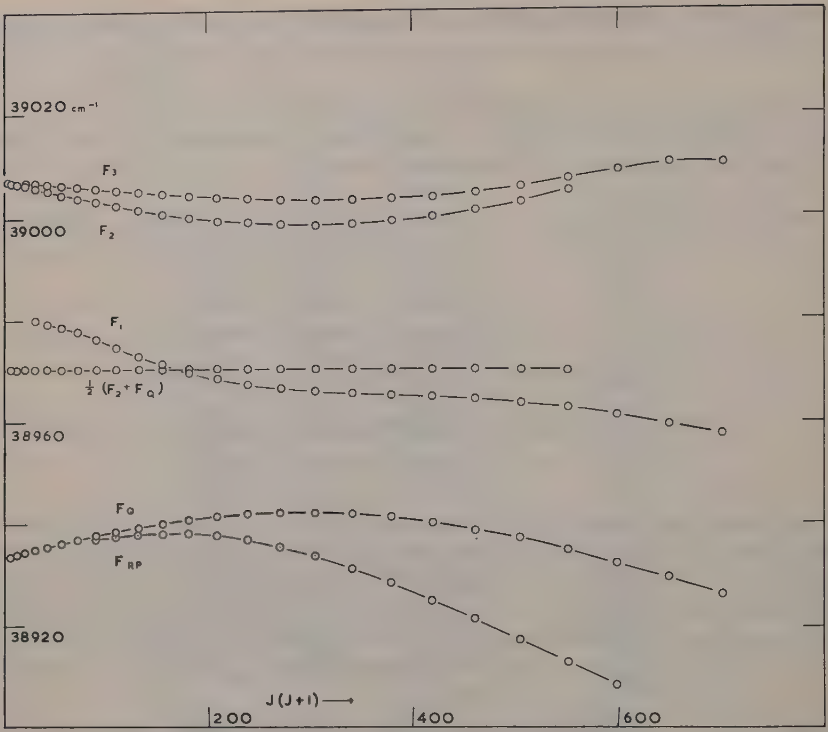

Fig. 9. $e\,^3\Sigma^-(v=e+1)$, $A\,^1\Pi\,(v=1)$: term values less $\frac{1}{2}\,(B_\Sigma + B_\Pi)\,J\,(J+1)$ plotted against $J\,(J+1)$.

This follows the conventions adopted for the discussion of the $^1\Pi$, $^3\Sigma^+$ interaction, except that for the low J-terms of $^1\Pi$, T_1 and T_2 have been interchanged.

Lines of all the eight branches expected for the $^3\Sigma^-, {}^1\Pi$–$^1\Sigma^+$ transition have been found, and unequivocal numberings can be given to the branches arising from T_1, T_3 and T_5 through the use of values of $\Delta_2 F''(J)$. Unfortunately the ^OP and ^QR branches which arise from the levels $T_3(^3\Sigma^-, F_1)$ are badly overlapped and it is possible that some details of the analysis here are incorrect. To number the Q and ^QQ branches which arise from T_2 and T_4 respectively, two assumptions are necessary: (i) the Q branch is numbered so that the limiting separation T_1–T_2 is zero at $J=0$ (see Table 4), (ii) the ^QQ branch is numbered so that $\frac{1}{2}\,(T_2+T_4) = \nu_0 + C/2 + \frac{1}{2}\,(B^*_\Sigma + B^*_\Pi)\,J\,(J+1)$ (see Fig. 9); i.e the influence of other perturbations on T_2 and T_4 is neglected. These numberings lead to a satisfactory value of B_Σ, and fit well with the observed structure (see Fig. 4).

The variation of $\Delta Q/2J$ with J is illustrated in Fig. 10: it will be seen that a further perturbation exists at $J \sim 28$. Constants were determined as for the $^1\Pi$, $^3\Sigma^+$ interaction. We obtain:

(i) With $B^*_\Pi = 0.7696$ cm^{-1}, from ref. [4], $B\,(^3\Sigma) = 0.6094$ cm^{-1}.
(ii) $2H = 56.2$ cm^{-1} (for $^1\Pi$, $3\,\Sigma^-$, F_2).

The relations (9) are also, of course, valid for a $^1\Pi$, $^3\Sigma^-$ perturbation: however of the relations (10), only (b), namely that $|T_2 - T_4| = 2\,|H\,(T^*_2,\,T^*_4)|$, holds

Table 4. Term values for $A\,^1\Pi$, $(v=1)$ and $e\,^3\Sigma^-$, $(v=e+1)$ referred to $J=0$, $v=0$ in $X\,^1\Sigma^+$.

		$^3\Sigma^-, F_1$ $J=N+1$		$A\,^1\Pi, F_{RP}$		$^3\Sigma^-, F_3$ $J=N-1$		$^3\Sigma^-, F_2$ $J=N$	$A\,^1\Pi, F_Q$
J	Branch	^QR	^OP	R	P	^SR	^QP	^QQ	Q
0									
1				39 834.50*	34.65*	39 908.35*	08.27	39 908.23	
2				37.38*	37.35*	10.92*	10.96	10.73	39 837.53
3				41.89	41.93	14.98*	14.97	14.61	41.98
4				47.83*	47.78*	20.40*	20.33	19.71	47.88
5		39 900.56*	00.27	55.03*	55.09	26.93*	27.08	26.18*	55.29
6		07.70	07.96*	63.87*	63.97	35.10*	35.05	33.78*	64.08*
7		16.89*	16.64*	74.14*	74.09	44.40*	44.42*	42.75*	74.44
8		26.85	26.80	85.57*	85.69	55.04*	55.16	53.07*	86.23
9		37.73	37.66	98.64*	98.70	67.17*	67.26	64.72	99.41
10		49.80	49.88	912.89*	12.95	80.64	80.64	77.63	914.00
11		63.34	63.26*	28.55*	28.49	95.58	95.46*	92.06*	29.89*
12		78.32	78.43*	45.23	45.24	40 011.61	11.65	40 007.77	47.29*
13		94.58*	94.80*	63.02*	63.03	29.10*	29.08*	24.94*	65.91*
14		40 012.62	12.59*	82.03	82.02	48.13*	48.11	43.60*	85.76*
15		32.21	32.20*	40 001.83	01.78*	68.53	68.47	63.82	40 006.94
16		53.33*	53.41*	22.39	22.50*	90.27*	90.35	85.49	29.30
17		76.34	76.29	44.21*	44.07	113.54	13.59	108.84	52.65
18		100.64	00.71	66.48*	66.38	38.44	38.43	33.94*	77.24*
19		26.56	26.56	89.77	89.69	64.89*	65.00*	60.58	102.77
20		53.70	53.77	113.80*	13.95*	92.87*	92.93	89.04	29.24
21		82.30*	82.16	39.19	39.10*	222.60	22.61	219.26	56.84*
22		211.53*	11.71	65.45	65.50	54.00	54.12*	51.12*	85.69
23		42.39	42.44	92.73*	92.67	87.19	87.19	84.92*	214.81
24		73.89*	74.10	221.23	21.12	321.92	22.00*		45.27
25		307.01*	06.87			57.80	57.74		76.81
26		40.60*	40.66			93.52	93.51*		309.29
27						443.44*			42.95*
28						82.38	82.44*	481.58	76.55*
29						524.80*	24.80	524.08*	411.54
30						69.45	69.78*	68.78*	
31						616.04*	15.94	615.29	
32						63.89*	63.92	63.41	
33						713.44*	13.32	713.04	
34						64.18	64.14	63.86	
35						816.17	16.26	815.92	
36						69.45*	69.34	69.01	

in the particular case of $A\,^1\Pi(1)$, $e\,^3\Sigma^-(e+1)$, because the perturbing matrix elements are so large that the interactions (T_1^*, T_3^*) and (T_1^*, T_5^*) strongly influence the terms involved. This can be seen from Fig. 9 in which are plotted the term values, less $\frac{1}{2}[B^*(^1\Pi)+B^*(^3\Sigma^-)]\,J(J+1)$, against $J(J+1)$.

(iii) From eq. (5) $C=47.8$ cm^{-1}.

(iv) We have using (11a), ν_0, $^1\Pi(1)=39\,833.1_0$ cm^{-1}. The limiting shift at $J=0$, from (6), is $\varepsilon=13.0_1$ cm^{-1}. Thus $\nu_0^*=39\,833.1+13.0=39\,846.1$ cm^{-1}. From

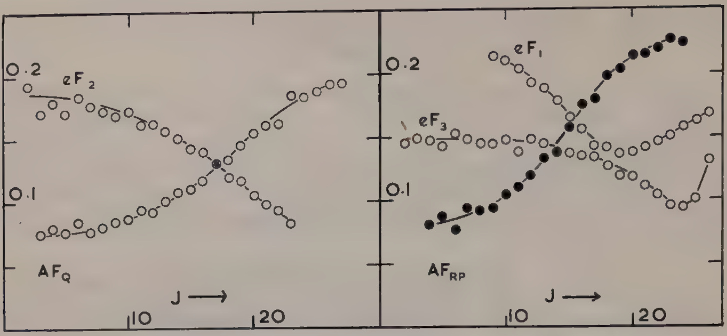

Fig. 10. $e\,^3\Sigma^-$ $(v=e+1)$, $A\,^1\Pi$ $(v=1)$: values of $\Delta Q/2J$ and of $(\Delta R+\Delta P)/4J$ plotted against J (equation 2).

(11a), we obtain $B_\Pi = 0.741_7$ cm^{-1}: the correction to this value, given by (3) is 0.0283 cm^{-1}, so that $B^*_\Pi = 0.741_1 + 0.0283 = 0.769_4$ cm^{-1}, in satisfactory agreement with the value obtained in ref. [4].

(v) ν^*_0, $e\,^3\Sigma^-(e+1) = \nu^*_0$, $A\,^1\Pi\,(1) + C = 39\,846.1 + 47.8 = 39\,893.9$ cm^{-1}.

The level $v'=1$ in $A\,^1\Pi$ is perturbed by several states besides $e\,^3\Sigma^-(e+1)$. Thus at $J \sim 28$ another perturbation appears both in the P and R and in the Q branches: the perturbing state has not been identified. At $J = 38.5$ (see 1) an interaction occurs with $a^*\,\Pi\,(a^*+2)$. As is shown below, this interaction is rather strong, and leads to a correction to ν_0 of $A\,^1\Pi\,(1)$ of about 1.5 cm^{-1}. At still higher J values $\sim$44–50, there is an interaction with $a'\,^3\Sigma^+\,(a'+2)$.

It is believed that these interactions may be responsible for one surprising feature of the present analysis. The triplet splitting in the level $v=e+1$ would be expected to be about the same as that in $v=e$, where (see below) $4\lambda + 2\gamma \sim +7$ cm^{-1}. However from the low J lines in $e+1$ one obtains $4\lambda + \gamma \sim +11$ cm^{-1}. This suggests that the effects of other perturbations on these levels cannot in fact be neglected.

Band $e\,^3\Sigma^-(e)$–$X\,^1\Sigma^+(0)$

At 2552 Å (39 170) cm^{-1}) lies a very weak band which analysis shows to be the e–0 band of the transition $e\,^3\Sigma^-$–$X\,^1\Sigma^+$. Lines of all all the five branches possible for this type of transition (see ref. [1]) have been found. Term values are given in Table 5. A small perturbation occurs at $J \sim 15.5$ in the ^QQ branch. The numbering in this branch after the perturbation is uncertain. Values of B^*_Σ and of ν^*_0 were derived from the ^QQ lines at low J before the perturbation. The spin-splitting constants were determined from T_3, T_4 and T_5 in the usual way. We obtain:

$$B^*\,(^3\Sigma^-, e) = 0.6134 \text{ cm}^{-1},$$
$$\nu^*_0\,(^3\Sigma^-, e) = 39\,160.8 \text{ cm}^{-1},$$
$$4\lambda + 2\gamma = 7.0 \text{ cm}^{-1}.$$

Bands $a^*\,\Pi$–$X\,^1\Sigma^+(0)$

A well-marked progression of three red-degraded bands at 2588.8, 2538.9 and 2492.2 Å (38 610, 39 370 and 40 110 cm^{-1}) appears in the absorption spectrum,

Table 5. Term values for $e\,^3\Sigma^-\,(v=e)$, referred to $J=0$, $v=0$ in $X\,^1\Sigma^+$.

N	Level	F_1		F_2	F_3	
	J	$N+1$		N	$N-1$	
	Branch	^QR	^OP	^QQ	^SR	^QP
0						
1				39 162.02*		
2				64.35		
3				68.17	67.43	
4		39 171.89*	71.56	72.97	71.99	71.89*
5		77.48*	77.74	79.23	77.53*	77.48*
6		84.89*	84.57	86.57	84.87*	84.89*
7		93.52*	93.92	95.03	93.53*	93.52*
8		203.20*	02.88*	204.88	203.34*	03.20*
9		14.11*	14.09	15.93	14.28*	14.11
10		26.53*	26.75	28.23	26.54*	26.53*
11		39.96*	39.90*	41.73	40.07	39.96*
12		54.64*	54.88*	56.55	54.75	54.64*
13		70.64*	70.56	72.54	70.65	70.64*
14		87.77*	87.82	89.84*	87.82*	87.77*
15		306.07	06.21	309.04	307.03	07.03
16		25.57	25.73	27.33		
17		46.68	46.59	48.30*		
18		68.69		70.51*		
19				93.65		
20				418.28		
21				44.07		
22				71.08		
23				99.29		
24				528.69		
25				59.38		
26				91.13		

and indeed the rather strong band at 38 610 cm^{-1} is a characteristic feature of this spectrum, even under low dispersion. The bands possess simple P, R and Q branches as in a $^1\Pi$–$^1\Sigma^+$ transition. Term values are given in Table 6. The observation of the lines $R(0)$ and $Q(1)$ in the a^*–0 band shows that the lowest level in a^* has $J=1$. Λ-type doubling is negligibly small. The structure is thus equally consistent, either with a $^1\Pi$–$^1\Sigma^+$ or with a $^3\Pi_1$ (case a, or case c)–$^1\Sigma^+$ transition. We therefore describe the state simply as $a^*\,\Pi$: both the multiplicity and the vibrational numbering remain to be determined.

Values of the constants for the state $a^*\,(\Pi)$ have been determined from the term values in the usual way (see Table 7).

Although no marked perturbations have been detected at $J<30$, the constants do not vary with v in the normal manner: in particular, the variation of D with v is anomalous. These effects result from interactions with other electronic states. The level $v=a^*$ is perturbed by $A\,^1\Pi\,(0)$: this interaction increases with decreasing J, so that the observed constants B_{e*} and D_{a*} are respectively bigger than B^*, D^*. The level a^*+2 interacts rather strongly with $A\,^1\Pi\,(1)$. The culmination of this perturbation (ref. [4]) lies at about $J\sim 38.5$. From the differences in the term values, obtained from lines given in ref. [4] we find $2H\sim 40$ cm^{-1}. With $C\sim 265$

Table 6. Term values for $a^*\Pi$, referred to $J=0$, $v=0$ in $X\,^1\Sigma^+$.

J	Band	a^*-0		$(a^*+1)-0$			$(a^*+2)-0$		
	Branch Q	R	P	Q	R	P	Q	R	P
1	38 615.07	15.05	14.98						
2	17.65	17.59*	17.70					14.95*	
3	21.29*	21.25*	21.31					18.75*	
4	26.42	26.16*	26.34	39 385.20*	85.18	84.87*	40 123.43	23.66	
5	32.58	32.69*	32.59	91.11*	91.38	91.05*	29.53	29.66*	29.69
6	40.09	40.09	40.08	98.57	98.59	98.30*	36.90	36.78	36.92
7	48.92	48.85	48.82	406.95	07.16	06.76*	45.31	45.21	45.28
8	58.83*	58.83	58.76	16.83	16.83	16.65*	54.96	54.82	55.03
9	70.07	70.20*	70.02	27.79	27.68*	27.83	65.89	65.93	66.05
10	82.49	82.54	82.54	40.04	40.13*	40.02	77.97	77.90	77.98
11	96.29	96.26	96.22	53.47	53.49	53.40	91.21	91.31	91.32
12	711.22	11.18	11.29	68.16	68.11*	68.00	205.73	05.86	05.71
13	27.35	27.44*	27.46	84.02	84.09*		21.51	21.49	21.59
14	44.81	44.88	44.84	501.05	01.11*	01.19	38.44	38.49	38.49
15	63.47	63.55	63.48	19.40	19.48*	19.30	56.68	56.72	56.69
16	83.41	83.40	83.39	38.89	39.14*	38.97	75.61	75.60	75.57
17	804.62	04.56	04.60	59.62	59.62	59.70	96.34	96.38	96.28
18	26.92	26.84	26.90	81.74	81.86	81.73	318.16	18.17	18.02
19	50.48	50.50	50.45	604.72	05.03	04.75	41.13	40.86	40.96
20	75.29	75.25	75.31	28.25	29.18	29.19	65.33	65.37	65.12
21	901.38	01.35	01.42	54.77	54.98*	54.77	90.61	90.67	
22	28.65	28.60	28.62	81.43	81.69	81.58	417.23	17.19	17.14
23	57.06	57.09	57.08	709.62	09.52	09.65	45.00	45.03	44.98
24	86.81	86.79	86.71	38.83	38.75		74.01	74.00	
25	39 017.69	17.64	17.56	69.24	69.20		504.19	04.19	
26	49.77	49.63		800.91	01.04		35.73	35.83	
27	83.21	83.05		33.79	33.81		68.28	68.23	
28	17.62	17.73		67.91	67.75		602.11	02.24	
29	53.44	53.53		903.02	03.27		37.17	37.22	
30					39.56		73.70	73.58	
31								30.45	

cm^{-1}, $\varepsilon \sim 1.7$ cm^{-1}, using (6). The anomalous value $D \sim 0$ for a^*+2 is explained by this perturbation, for, on approaching the perturbation from low values of J, the effective value of $B(a^*+2)$ increases, so that the observed value of D is fortuitously zero. From the values of ε and C given above, $B^*(a^*+2) \sim 0.604 - 0.0007 \simeq 0.603$ cm^{-1}. In agreement with the suggestion that the least perturbed level is a^*+1 is the fact that for this level the observed value of D agrees best with that calculated from Kratzer's relation (1.6×10^{-6} cm^{-1}).

Summary and discussion

The constants derived in the present work are summarized in Table 7.

Eight interactions between $a'\,^3\Sigma^+$ and $A\,^1\Pi$ and six between $e\,^3\Sigma^-$ and $A\,^1\Pi$ were recognized in [4]. The observation of the levels a^*, a^*+1, a^*+2 in absorption leads to the identification of two further perturbations, namely a^*+2, $A\,^1\Pi(1)$ at $J=39.5$ and a^*+5, $A\,^1\Pi(3)$ at $J=37.5$. There remain seven interactions observed in [4] and the perturbation at $J=15.5$ in $e\,^3\Sigma^-(e)$. At least six

Table 7. Summary of band constants.

Values in parentheses have been taken from ref. [4].

State	v	ν_0^*	B^*	$10^6 D$
$A\,^1\Pi$	0	38 797.6	0.7768	
	1	39 847.8	0.7694	
	2	40 884.5	(0.7617)	(1.62)
$a^*\,\Pi$	a^*	38 613.9	0.6248	5
	a^*+1	39 372.9	0.611	2
	a^*+2	40 109.7	0.603	0
$a'\,^3\Sigma^+$	a'	38 851.8	0.5836	
	$a'+3$	40 988	(0.559)	
$e\,^3\Sigma^-$	e	39 160.8	0.6134	
	$e+1$	39 893.9	0.6094	

of these have the characteristics of a singlet–singlet interaction, appearing in the R, P and Q branches at the same J value. The B values of the perturbing levels, B_p, are in all cases smaller than those of the levels which they perturb. Assuming that the values of B_p be within the range 0.55 to 0.8 cm^{-1}, these levels are found to fall into a pattern such as would be given by successive vibrational levels of two electronic states. We call these states x and y. Little is yet known about these states, although one of them is probably a $^1\Delta$ (or a $^1\Pi$) state. Constants for all the known states of CS are collected in Table 8.

It must be emphasized that when so many states interact with one another, it is quite impossible to derive adequate corrections, either to ν_0 or to B, in the absence of complete information about the perturbing matrix elements and molecular constants for all the perturbing states. Derived values of the smaller constants, particularly $x_e\,\omega_e$ and α, may therefore be very uncertain.

The present study of the absorption of CS has revealed the existence of one new excited state, $a^*\,\Pi$, and has confirmed in a very striking way the existence of the two triplet states, $a'\,^3\Sigma^+$ and $e\,^3\Sigma^-$, which had earlier been indentified only through their interactions with $A\,^1\Pi$. The directly determined constants for these triplet states agree statisfactorily with those derived earlier from the analysis of the perturbations.

The expected low-lying configurations are

(1) $(z\sigma)^2\ (y\sigma)^2\ (w\pi)^4\ (x\sigma)\ (v\pi)$, $^1\Pi$, $^3\Pi_r$,

(2) $(z\sigma)^2\ (y\sigma)^2\ (w\pi)^3\ (x\sigma)^2\ (v\pi)$, $^1\Sigma^+$, $^1\Sigma^-$, $^3\Sigma^+$, $^3\Sigma^-$, $^1\Delta$, $^3\Delta$,

and there seems little doubt that state A corresponds to the $^1\Pi$ state arising from configuration (1), and that a' and e arise from (2). One problem which remains is the identity of the state $a^*\,\Pi$. The lowest excited state expected for CS is $^3\Pi_r$, and it is tempting to suggest that a^* is the $^3\Pi_1$ component of this state. If this is the case, then there should be observable at slightly longer wavelengths the transition $^3\Pi_{0+}$–$X\,^1\Sigma^+$: in fact, no lines which could be assigned to such a transition have been found. This does not however rule out the possibility that a^* is $^3\Pi$, for the relative intensities of bands in this spectrum

Table 8. Constants for the electronic states of CS.

State	T_o	ω_e	$x_e\omega_e$	B_e	$10^3\alpha_e$	r_e, Å
y	$T_y \sim 39\,950$	–	–	$B_y < 0.77$	–	–
x	$T_x \sim 39\,170$	–	–	$B_x < 0.61$	–	–
$e\,^3\Sigma^-$	$\leqslant 39\,160.8$	$\geqslant 742_5$	$4._7$	$\geqslant 0.617$	$6._5$	$\leqslant 1.77$
$a'\,^3\Sigma^+$	$\leqslant 38\,851.8$	$\geqslant 739$	$5._5$	$\geqslant 0.587$	8	$\leqslant 1.81$
$A\,^1\Pi$	38 797.6	$1073._4$	$10._1$	0.7800	6.3[a]	1.574
$a^*\,\Pi$	$\leqslant 38\,613.9$	$\geqslant 780$	10	$\geqslant 0.629$	11	$\leqslant 1.75$
$X^1\,\Sigma^+$	0	1285.08	6.46	0.82005	5.92	1.535

[a] $-0.0004\,(v+\frac{1}{2})^2$.

are highly unusual; for example, whereas the a'–0 and $(a'+3)$–0 bands are comparatively strong, the $(a'+1)$, $(a'+2)$–0 bands do not appear on the present plates. Thus the $^3\Sigma^-$–$^1\Sigma^+$ systems in CS borrow intensity from $A\,^1\Pi$–$X\,^1\Sigma^+$, and this may also be the case with $a^*\,\Pi$–X.

The increase of the observed intensity in the forbidden systems in going from CO to CS is indeed remarkable, as is shown by the estimate of relative intensity below:

	CO	CS
$A\,^1\Pi$–$X\,^1\Sigma^+$	1	1
$a'\,^3\Sigma^+$, $e\,^3\Sigma^-$–$X\,^1\Sigma^+$	$\sim 10^{-4}$	~ 0.1

These figures indicate that conclusions about the strengths of forbidden systems should be drawn only with extreme caution.

Finally, it may be noted that the structures observed in the forbidden transitions $^3\Sigma^\pm$–$^1\Sigma^+$ in CS are in exact agreement with those first analyzed in CO, and that the structure of the $^3\Sigma^+$, $^1\Pi$ interaction is also in exact agreement with theoretical prediction. In the case of the $^3\Sigma^-$, $^1\Pi$ interaction, this is not the case, and although the F_2 levels of the $^3\Sigma^-$ state run normally, the F_1 and in less degree the F_3 levels do not follow the expected pattern. It is just possible that the analysis here is incorrect in some details, but it seems more probable that the approximation of only two interacting states is inadequate in this particular instance.

A study of the absorption spectrum at higher path-lengths may provide the answers to some of these problems.

REFERENCES

1. Herzberg. G., and Hugo, T. J., Canad. J. Phys. *33*, 757 (1955).
2. Kovács, I., Canad. J. Phys. *36*, 309 (1958).
3. Lagerqvist, A., and Miescher, E., Helv. Phys. Acta *31*, 221 (1958).
4. Lagerqvist, A., Westerlund, H., Wright, C. V., and Barrow, R. F., Ark. f. Fys. *14*, 387 (1958).
5. Mockler, R. C., and Bird, R., Phys. Rev. *98*, 1837 (1955).

Tryckt den 8 december 1960

Uppsala 1960. Almqvist & Wiksells Boktryckeri AB